THE JOURNAL OF BIOLOGICAL CHEMISTRY
Vol. 273, No. 10, Issue of March 6, pp. 5771–5779, 1998
Printed in U.S.A.

Engineering of Cyclodextrin Product Specificity and pH Optima of the Thermostable Cyclodextrin Glycosyltransferase from *Thermoanaerobacterium thermosulfurigenes* EM1*

(Received for publication, June 9, 1997, and in revised form, October 8, 1997)

Richèle D. Wind‡§, Joost C. M. Uitdehaag¶, Reinetta M. Buitelaar‡, Bauke W. Dijkstra¶, and Lubbert Dijkhuizen‖

From the ‡Agrotechnological Research Institute (ATO-DLO), P. O. Box 17, 6700 AA Wageningen, ¶BIOSON Research Institute and Laboratory of Biophysical Chemistry, Groningen Biomolecular Sciences and Biotechnology Institute (GBB), University of Groningen, Nijenborgh 4, 9747 AG Groningen, and ‖Department of Microbiology, Groningen Biomolecular Sciences and Biotechnology Institute (GBB), University of Groningen, Kerklaan 30, 9751 NN Haren, The Netherlands

The product specificity and pH optimum of the thermostable cyclodextrin glycosyltransferase (CGTase) from *Thermoanaerobacterium thermosulfurigenes* EM1 was engineered using a combination of x-ray crystallography and site-directed mutagenesis. Previously, a crystal soaking experiment with the *Bacillus circulans* strain 251 β-CGTase had revealed a maltononaose inhibitor bound to the enzyme in an extended conformation. An identical experiment with the CGTase from *T. thermosulfurigenes* EM1 resulted in a 2.6-Å resolution x-ray structure of a complex with a maltohexaose inhibitor, bound in a different conformation. We hypothesize that the new maltohexaose conformation is related to the enhanced α-cyclodextrin production of the CGTase.

The detailed structural information subsequently allowed engineering of the cyclodextrin product specificity of the CGTase from *T. thermosulfurigenes* EM1 by site-directed mutagenesis. Mutation D371R was aimed at hindering the maltohexaose conformation and resulted in enhanced production of larger size cyclodextrins (β- and γ-CD). Mutation D197H was aimed at stabilization of the new maltohexaose conformation and resulted in increased production of α-CD.

Glu^{258} is involved in catalysis in CGTases as well as α-amylases, and is the proton donor in the first step of the cyclization reaction. Amino acids close to Glu^{258} in the CGTase from *T. thermosulfurigenes* EM1 were changed. Phe^{284} was replaced by Lys and Asn^{327} by Asp. The mutants showed changes in both the high and low pH slopes of the optimum curve for cyclization and hydrolysis when compared with the wild-type enzyme. This suggests that the pH optimum curve of CGTase is determined only by residue Glu^{258}.

Cyclodextrins (CDs)[1] are cyclic molecules composed of 6, 7, or 8 glucose units linked via α(1,4)-glycosidic bonds (α-, β-, and γ-CD, respectively). The ability of cyclodextrins to form inclusion complexes with small hydrophobic molecules has provided a number of practical uses in the food, pharmaceutical, and agrochemical industries (1–3). Cyclodextrins are produced from starch by the action of the enzyme cyclodextrin glycosyltransferase (CGTase; EC 2.4.1.19). However, apart from the cyclization reaction, the enzyme can also catalyze disproportionation, coupling, and hydrolysis reactions. All known CGTases produce a mixture of α-, β-, and γ-cyclodextrins. For the industrial production of pure cyclodextrins, β-CD is selectively crystallized and α- and γ-CD are complexed with organic solvents. The industrial production of cyclodextrins might be improved by the construction of mutant CGTases with improved product specificity (2, 3).

In the conventional commercial production of cyclodextrins, starch is first liquefied by the action of a thermostable α-amylase, whereafter cyclodextrins are produced using the mesophilic CGTase from *Bacillus macerans*. Two highly thermostable CGTases have been characterized that can directly be used for starch liquefaction, eliminating the need for α-amylase pretreatment (2, 3). These enzymes are produced by thermophilic anaerobic bacteria belonging to the genus *Thermoanaerobacter* (9, 10) and *Thermoanaerobacterium thermosulfurigenes* EM1 (11). The overall amino acid compositions of both enzymes show relatively minor differences, and also the biochemical characteristics of both enzymes are very similar (11). The *T. thermosulfurigenes* EM1 CGTase displays maximum cyclization activity at 80–85 °C and maximum starch hydrolyzing activity at 90–95 °C. The pH optimum for cyclization is broad, in the range of pH 4.5–7.0.

The three-dimensional structures of several CGTases have been solved (4, 5, 7). CGTase belongs to family 13 of the glycosyl hydrolases, a group of homologous $(\beta/\alpha)_8$-barrel proteins, to which also the α-amylases belong (8). Recently, the three-dimensional structure of the CGTase from *T. thermosulfurigenes* EM1 (*Tabium* CGTase) was solved at 2.3-Å resolution (6). In the present study we describe the three-dimensional structure of an enzyme-substrate complex of *Tabium* CGTase. The x-ray structure of a maltohexaose inhibitor complexed with *Tabium* CGTase was solved at 2.6-Å resolution. The detailed information thus obtained allowed rational engineering of the cyclodextrin product specificity of *Tabium* CGTase.

Residues Glu^{258}, Asp^{329}, and Asp^{230} are directly involved in catalysis in CGTase (20). Glu^{258}, together with Asp^{230}, is believed to cleave the substrate's α(1,4)-glycosidic bonds and to form the product's α(1,4)-glycosidic bonds by a double displacement mechanism (15). In the first step of the reaction the general acid Glu^{258} protonates the oxygen of the glycosidic

* This work was supported by European Community Grants AIR-CT-93-1023 (to R. D. W. and R. M. B.) and ERBIO2-CT-94-3071 (to J. U., B. W. D., and L. D.). The costs of publication of this article were defrayed in part by the payment of page charges. This article must therefore be hereby marked "*advertisement*" in accordance with 18 U.S.C. Section 1734 solely to indicate this fact.

§ To whom correspondence should be addressed: ATO-DLO, P. O. Box 17, 6700 AA Wageningen, The Netherlands. Tel.: 31-317-475321; Fax: 31-317-475347; E-mail: r.d.wind@ato.dlo.nl.

[1] The abbreviations used are: CD(s), cyclodextrin(s); CGTase, cyclodextrin glycosyltransferase; CAPS, 3-(cyclohexylamino)propanesulfonic acid; MBS, maltose binding site; PCR, polymerase chain reaction; HPLC, high performance liquid chromatography.

bond to be cleaved. After cleavage of this scissile bond, an oxocarbonium transition state is formed, which is believed to collapse into a covalently linked intermediate by nucleophilic attack of Asp^{230} on the anomeric C1. Subsequently, the reducing end diffuses out of the active site and an acceptor comes in, which can be a water molecule (in case of hydrolysis) or a carbohydrate C4-hydroxyl group (in case of transglycosylation). In the second step of the reaction, the acceptor hydroxyl group is activated through deprotonation by Glu^{258}, after which the acceptor performs a nucleophilic attack on the covalent intermediate. Through another oxocarbonium transition state, the product (α(1,4)-linked) is then formed (16, 17).

It appears from the double displacement mechanism that for optimal catalysis the nucleophile Asp^{230} must be deprotonated in the first step of the reaction, whereas the general acid Glu^{258} must be protonated in the first step, but deprotonated in the second step of the reaction. A third catalytic residue, Asp^{329}, has been found to be hydrogen bonded to Glu^{258} in the unliganded CGTase, thereby elevating the pK_a of Glu^{258} and assuring its protonation. After substrate binding, this hydrogen bond is lost, making deprotonation of Glu^{258} possible. It was suggested that this Glu^{258}-Asp^{329} interaction is responsible for the broad pH optimum exhibited by CGTases (16). The importance of the pK_a of Glu^{258} in the different reactions catalyzed by *Tabium* CGTase was further studied. By changing the electrostatic environment of Glu^{258} by site-directed mutagenesis, we could drastically shift the *Tabium* CGTase pH optimum.

The biochemical characteristics of the various mutant CGTases are presented with emphasis on the effects of these mutations on the CGTase cyclization and hydrolytic activities, pH optima, and product formation from starch.

EXPERIMENTAL PROCEDURES

Structure Determination—Crystals of the *Tabium* CGTase were grown from 21% saturated ammonium sulfate in 100 mM Tris buffer, pH 7.6. The crystals were stable in the presence of carbohydrates.

A double soaking experiment was started identical to that described earlier for the *Bacillus circulans* strain 251 CGTase (13). A *Tabium* CGTase crystal was soaked for 20 min in a solution of 0.25% w/v acarbose in 21% saturated ammonium sulfate and 100 mM CAPS buffer, pH 9.8, followed by 7 days of soaking in a solution of 0.5% maltohexaose in 21% saturated ammonium sulfate in 100 mM CAPS buffer, pH 9.8.

Data were collected to a resolution of 2.6 Å on a MacScience Dip2000K Image Plate system and processed with XDS (23). Refinement of the structure was done with the TNT package (24), using the 2.3-Å structure of unliganded *Tabium* CGTase as a starting model (6). Rigid body refinement was followed by coordinate and all parameter (coordinates and individual atomic temperature factors) refinement. A test set for calculating a free *R* factor (25) comprised 8% (1956) of the unique reflections. Ideal protein bond lengths and angles were taken from Engh and Huber (26), ideal bond lengths and angles for glucose were taken from the crystal structure of maltose (27). Planarity, van der Waals contacts, and B factor correlations were restrained, whereas torsion angles were not. Chiral centers were watched. The model was manually adjusted using O (28), running on a Silicon Graphics workstation, in combination with the program OOPS (29). Electron density was displayed using σ_A weighted $F_o - F_c$, $2F_o - F_c$ maps, and omit difference maps (30, 31).

In the course of the refinement, density appeared for 6 glucose units in the active site, at subsites −3, −2, −1, 1, 2, and 3. In this naming convention, the glycosidic bond between −1 and 1 is the scissile bond, and the substrate reducing end is at position −3. In previous structures with acarbose and the acarbose derived maltononaose inhibitor (13, 16), the valienamine moiety of acarbose was located at subsite 2 and the 6-deoxyglucose group at subsite 1. This time, clear omit $F_o - F_c$ density showed up at the 6-hydroxyl position at subsite 1, even after thorough refinement with a hexakis 6-deoxymaltohexaose as a carbohydrate model in the active site. Refining with maltohexaose as a model removed the difference density at position 1 completely. We decided to model a valienamine group, which has a 6-OH group, at subsite 1, and according to the acarbose structure, 6-deoxyglucose at subsite −1. This resulted in the *N*-glycosidic linkage of acarbose being positioned at the site of hydrolytic cleavage. This binding mode of acarbose in the active site is also observed in related α-amylases (32). At subsites −2 and +2 electron density indicated the presence of 6-OH groups, so glucoses were modeled in. Furthermore, also at subsites −3 and +3 glucoses were placed, resulting finally in an acarbose derived maltohexaose in the active site of CGTase.

TABLE I
Data collection and final model quality

Protein	*Tabium* wild-type
Soaked with	Acarbose + maltohexaose
Temperature	298 K
Cell ($P2_12_12_1$):	
a (Å)	116.2
b (Å)	97.79
c (Å)	74.00
Resolution range (Å)	45.0–2.56
Total observations	181,769
Discarded observations	30,645
Unique reflections	25,423
R_{merge} (%)	6.82
Completeness (%)	91.1
Completeness (%) in the last resolution shell (Å)	74.3 (2.60–2.56)
No. of protein atoms	5333
No. of calcium atoms	2
No. of carbohydrate atoms	101
No. of solvent sites	185
Average *B* factor (Å^2)	17.9
Final R factor (%)	18.6
Final free R factor (%)	25.5
Root mean square deviation from ideality:	
Bond lengths (Å)	0.003
Bond angles (deg)	0.974
Torsion angles (deg)	17.512
Trigonal planes (Å)	0.007
Planar groups (Å)	0.007
van der Waals contacts (Å)	0.010
B factor correlations (Å^2)	1.573

Solvent molecules were taken from the 2.3-Å *Tabium* structure (6), and runs of the program ARP (33) were used to add and remove water molecules with bad electron density. Finally, water molecules with bad density, *B* factors larger than 50 Å^2, or no hydrogen bonds were removed by hand. Furthermore, at a binding site distant from the active site, equivalent to maltose binding site 3 (MBS3) in *BC251* CGTase (5), density for a maltotriose was found, which was subsequently modeled in. MBS1 and MBS2 of *BC251* CGTase (5) were not occupied in *Tabium* CGTase.

The final model was analyzed with the PROCHECK package (34). It contained all 683 amino acids, 2 Ca^{2+}, an acarbose-based maltohexaose inhibitor in the active site, a maltotriose at MBS3, and 185 solvent oxygens. Refinement details and statistics can be found in Table I.

Bacterial Strains, Plasmids, and Growth Conditions—Escherichia coli JM109 (35) was used for recombinant DNA manipulations. *E. coli* PC1990 (36), known to leak periplasmic proteins into the supernatant because of a mutation in its *tolB* locus, was used for (extracellular) production of CGTase (mutant) proteins. Plasmid pCT2, a derivative of pUC18 containing the *amyA* (*cgt*) gene of *T. thermosulfurigenes* EM1 (37), was used for site-directed mutagenesis, sequencing, and expression of the CGTase (mutant) proteins (Fig. 1). Plasmid-carrying bacterial strains were grown on LB medium with 100 μg/ml ampicillin. When appropriate, isopropyl-β-D-thiogalactopyranoside was added at a concentration of 0.1 mM for induction of protein expression.

DNA Manipulations—DNA manipulations and transformation of *E. coli* were essentially as described by Sambrook *et al.* (38). Electrotransformation of *E. coli* was performed using the Bio-Rad gene pulser apparatus (Bio-Rad, Veenendaal, The Netherlands). The selected conditions were 2.5 kV, 25 μF, and 200 Ω.

Site-directed Mutagenesis—Mutant CGTase genes were constructed via a double PCR method using *Pfu* DNA polymerase (Stratagene, Westburg, Leusden, The Netherlands). A first PCR reaction was carried out with the mutagenesis primer for the coding strand plus a primer 195–715 base pairs downstream on the template strand. The reaction product was subsequently used as primer in a second PCR reaction together with a primer 295–815 base pairs upstream on the coding strand. The product of the last reaction was cut with *Nco*I and *Mun*I

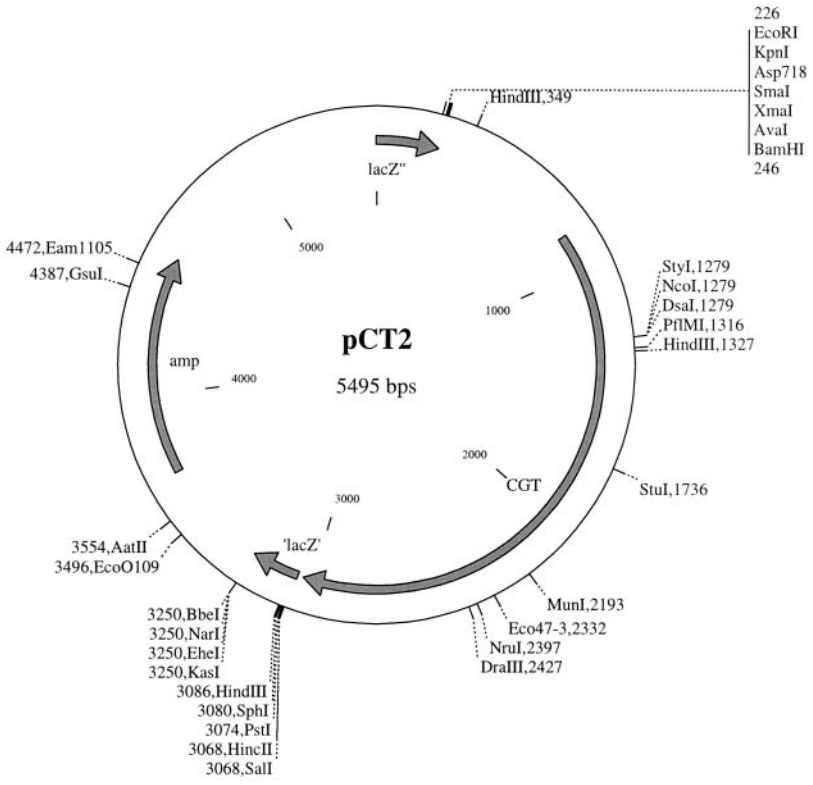

FIG. 1. **Restriction map of the plasmid pCT2.**

and exchanged with the corresponding fragment (900 base pairs) from the vector pCT2 (Fig. 1). The resulting (mutant) plasmid was transformed to *E. coli* JM109 for sequencing and to *E. coli* PC1990 for production of the (mutant) proteins. The following oligonucleotides were used to produce the mutations: D197H, 5′-CGTAACTTATT-T**CAT**TTAGCAGATCTAAATCAACAG-3′; F284K, 5′-GTCTTTTGGA-C**AAG**AGGTTTTCTC-3′; N327D, 5′-GGTTACTTTTATTGAT**GAT**CA-TGATATGG-3′; D371R, 5′-GACAGGCAATGGA**CGT**CCTTATAATA-GAGC-3′. The bold codons indicate the changed amino acids. Successful mutagenesis resulted in appearance of the underlined restriction sites (*Bgl*II for D197H, *Bcl*I for N327D and *Aat*II for D371R), which allowed rapid screening of potential mutants. It was not possible to find a convenient restriction site for mutant F284K. Mutations were verified by DNA sequencing (39). All 900 base pairs on the *Mun*I-*Nco*I fragment obtained by PCR were checked by DNA sequencing.

Production and Purification of CGTase Proteins—For production of CGTase proteins, *E. coli* PC1990 (pCT2) was grown in a 2-liter fermentor at pH 7.0 and 30 °C. The medium contained 2% (w/w) trypton (Oxoid, Boom BV, Meppel, The Netherlands), 1% (w/w) yeast extract (Oxoid), 1% (w/w) sodium chloride, 1% (w/w) casein hydrolysate (Merck, Darmstadt, Germany), 100 μg/liter ampicillin, and 0.1 mM isopropyl-β-D-thiogalactopyranoside. Growth was monitored by measuring the absorbance (A) at 450 nm. At an $A_{450\ nm}$ of 2–3, an extra amount of 50 g of trypton was added to the fermentor. Cells were harvested after 20–24 h of growth (8000 × g, 30 min, 4 °C), at absorbance values of 8–12. The supernatant was directly applied to an α-CD-Sepharose-6FF affinity column (40) for further purification of the CGTase proteins. After washing the column with 10 mM sodium acetate, pH 5.5, the CGTase was eluted with the same buffer supplemented with 1% (w/w) α-CD. Purity and molecular weight of the CGTase (mutant) proteins were checked on SDS-polyacrylamide gel electrophoresis (11). Protein concentrations were determined by the method of Bradford (42), using the Coomassie protein assay reagent of Pierce (Pierce Europe bv, Oud-Beijerland, The Netherlands).

Enzyme Assays—Specific assays were used to determine the activities (initial rates) of the four different reactions catalyzed by CGTases (14). In the cyclization reaction the reducing end of a sugar is transferred to another sugar residue in the same oligosaccharide chain, resulting in the formation of cyclic compounds. Coupling is the reverse reaction in which a cyclodextrin molecule is linked to a linear oligosaccharide chain, producing a longer oligosaccharide chain. In the disproportionation reaction, part of a linear donor-oligosaccharide is transferred to a linear acceptor chain. The saccharifying activity is the hydrolysis of starch into linear oligosaccharides. All assays were standardly performed at pH 6.0 and 60 °C. Cyclization and saccharifying assays were performed as described by Penninga *et al.* (14). Coupling activity was measured essentially as described by Nakamura *et al.* (41). β-CD (2.5 mM) was used as donor substrate and methyl α-D-glucopyranoside (100 mM) as acceptor substrate. The linear oligosaccharide formed in the reaction was converted to single glucose units by the action of amyloglucosidase (Sigma, Darmstadt, Germany). Glucose was detected with the glucose/GOD-Perid method of Boehringer Mannheim (Almere, The Netherlands). Disproportionation activity was measured as described by Nakamura *et al.* (18). EPS, 4-nitrophenyl-α-D-maltoheptaoside-4–6-*O*-ethylidene (3 mM, Boehringer Mannheim), was used as donor substrate and maltose (10 mM) as acceptor substrate. The reaction product containing the nitrophenyl group was cleaved by the action of α-glucosidase (Boehringer Mannheim). For each reaction units were defined as the amount of enzyme producing/converting 1 μmol of product/substrate at pH 6.0 and 60 °C.

The pH optimum for cyclization was determined by incubating 0.1 units/ml (β-CD forming activity) of the enzyme with 5% Paselli SA2 (partially hydrolyzed potato starch; AVEBE, Foxhol, The Netherlands) in a 10 mM sodium citrate solution set at a specific pH (range 4.0–8.0). For each pH a new calibration curve was prepared with 0–2 mM β-CD. The pH optimum for the saccharifying reaction was determined in a similar way.

HPLC Product Analysis—Formation of cyclodextrins was measured under industrial process conditions by incubation of 0.1 unit/ml CGTase (β-CD forming activity) with 10% Paselli WA4 (pregelatinized drum-dried starch with a high degree of polymerization; AVEBE) in 10 mM sodium citrate buffer, pH 6.0, at 60 °C for 45 h. Samples were taken at regular time intervals and boiled for 10 min. Products formed were analyzed by HPLC, using a 25-cm Econosil-NH_2 10-μm column (Alltech Nederland bv, Breda, The Netherlands) eluted with acetonitrile/water (65:45) at 1 ml/min. Products were detected by a refractive index detector (Waters 410, Waters Chromatography Division, Milford, MA). The temperature of the flow cell and column was set at 50 °C, to avoid possible precipitation of starch. Formation of linear products was directly analyzed. Formation of CDs was analyzed after incubation of the samples with an appropriate amount of β-amylase (type I-B from sweet potato, Sigma, Boom BV, Meppel, The Netherlands), degrading linear sugars (but not CDs) to glucose. The retention times for α-, β-, and γ-CD were the same as those for G4, G5, and G6 linear oligosaccharides, respectively.

FIG. 2. **Conformation of the maltohexaose inhibitor in the active site of the CGTase from *T. thermosulfurigenes* EM1.** The inhibitor is occupying subsites −3 to +3 in domains A and B of the CGTase.

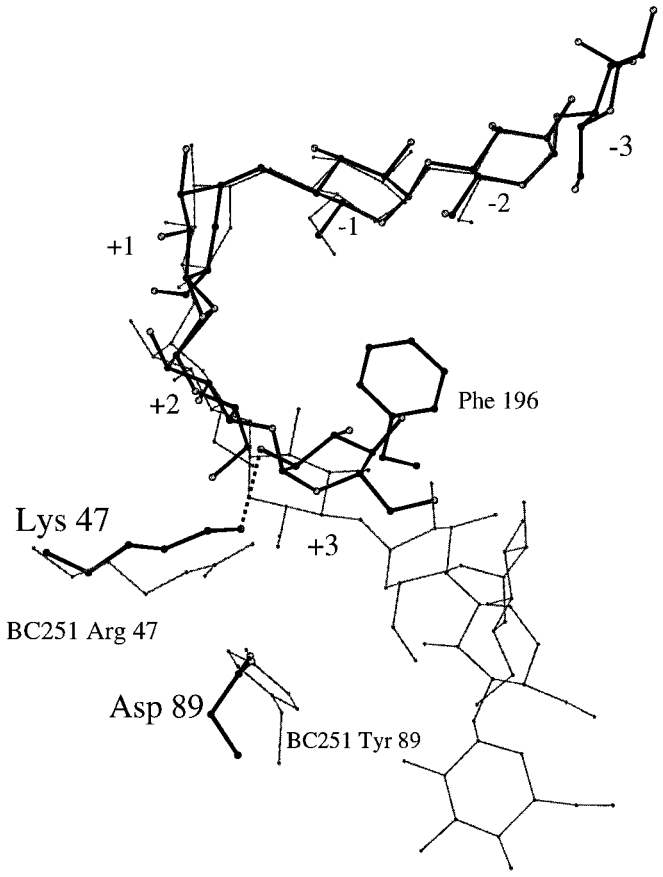

FIG. 3. **Superposition of the maltohexaose (*sticks*) and maltononaose (*lines*) inhibitor structures.** At subsite +3 the conformation of the maltohexaose inhibitor is more bent toward Phe[196] and is stabilized by Lys[47], which is Arg[47] in the CGTase from *B. circulans* strain 251. Moreover, the replacement of Tyr[89] (*B. circulans* CGTase) by Asp[89] (*T. thermosulfurigenes* EM1 CGTase) makes that the "straight" maltononaose conformation at subsite +3 is not as stably bound in *T. thermosulfurigenes* EM1 CGTase than as in *B. circulans* CGTase.

RESULTS AND DISCUSSION

Binding of the Maltohexaose Inhibitor

The maltohexaose inhibitor complexed with the CGTase from *T. thermosulfurigenes* EM1 was bound at subsites −3 to +3 (Fig. 2). In complexes with *BC251* CGTase (13) or other CGTases, binding at subsite −3 has never been observed. The present study thus reveals the nature of subsite −3 for the first time. The glucose at subsite −3 (overall *B* factor: 58 Å^2) has long distance interactions with Glu[264] O-ϵ1 and Thr[262] N, both at 3.6 Å. A better contact is formed at 3.4 Å with the Asn[591] Oδ1 from a symmetry related molecule. This stabilization by a crystal contact may explain why in *BC251* CGTase crystals a glucose at subsite −3 has never been observed. The interactions that do not result from a crystal contact are very weak, indicating that subsite −3 is not of large relevance.

In the vicinity of the scissile bond the active site architecture is identical in *Tabium* and *BC251* CGTase. It is therefore not surprising that at subsites −2 to +2, the maltohexaose inhibitor is bound in the same fashion to *Tabium* CGTase as the maltononaose inhibitor to *BC251* CGTase (13). Even though the acarbose binding mode has been modeled differently, the same amino acids are providing similar interactions from subsites −2 to +2, suggesting that acarbose can adapt its conformation easily to that required by the active site. It is clear that differences in characteristics between *Tabium* and *BC251* CGTase must originate from interactions at more distant subsites.

In contrast to subsites −2 to +2, at subsite +3 the binding mode of the maltohexaose inhibitor is radically different from the maltononaose binding mode, the former being more bent. In Fig. 3, an overlay of the two inhibitor conformations can be seen. All enzyme-substrate interactions are given in Table II. The glucose at subsite 3 of the maltohexaose inhibitor occupies a position more bent toward Phe[196]. This conformation at subsite 3 is stabilized by Lys[47]. In *BC251* CGTase this residue is Arg[47], which so far has never been found to be involved in substrate binding. Furthermore, in the *BC251* enzyme Tyr[89] has strong interactions at subsite 3, but in the *Tabium* CGTase this residue is an Asp. The conformation of Asp[89] does not allow any interactions with substrate. Apart from these two differences at subsite 3, residues in *Tabium* CGTase at subsites 4–7 might be unfavorable to the maltononaose binding mode (straight), although we could not find evidence for that from the structure of *Tabium* CGTase. The maltohexaose conformation observed is only stabilized by the protein through the contact with Lys[47]. The maltohexaose conformation, however, might have less internal strain because it allows the O2–O3 interglucoside hydrogen bond between subsites 2 and 3 to be formed at 2.7 Å, whereas in the straight conformation the O2–O3 distance is 4.0 Å (13) prohibiting hydrogen bond formation. In addition, the lack of interactions with the enzyme might allow for more flexibility of the maltohexaose chain, which would thus be entropically stabilized. On the basis of these data, we thought it possible to favor one binding mode over the other by site-directed mutagenesis, thereby investigating whether it could be related to one of the *Tabium* CGTase characteristics.

The *Tabium* and *BC251* CGTases are different in many respects. The molecular basis for thermostability of the *Tabium* CGTase has been extensively discussed (6). Furthermore, *Tabium* CGTase displays a relatively high hydrolytic activity (24 units/mg), compared with *BC251* CGTase (3.5 units/mg), which results in formation of substantial amounts of linear

sugars besides cyclodextrins from starch (11). *Tabium* CGTase produces a mixture of α-, β-, and γ-CD at a ratio of 28:58:14, respectively, whereas *BC251* CGTase has a product ratio of 13:64:23 (14). A mutant *BC251* CGTase with a substantially higher α-cyclodextrin production also showed preference for a bent maltohexaose inhibitor over a straightly bound maltononaose inhibitor (43). This suggests a relation between the bent conformation and α-cyclodextrin production. The maltohexaose and maltononaose binding modes thus may reflect (part of) specific intermediates for α-CD and β-CD production by *Tabium* CGTase and *BC251* CGTase, respectively. Further experimental evidence for this was sought by modifying relevant residues in *Tabium* CGTase, using site-directed mutagenesis. Since the maltohexaose and maltononaose inhibitors are synthesized by CGTase *in situ* in the crystal, no sufficient quantities were available to determine their binding or inhibitor constants. Therefore we designed our mutants only by qualitative arguments.

TABLE II
Interactions of a maltohexaose inhibitor with T. thermosulfurigenes CGTase

Stack indicates an aryl-carbohydrate stacking interaction; w.m., water-mediated contact; distances are specified for putative hydrogen bonds or other electrostatic interactions.

Maltohexaose inhibitor	Glucoside atom	*Tabium* residue	Distance
			Å
Subsite -3	O3	Glu^{265} O-ε1	3.6
	O2	Thr^{263} N	3.6
Subsite -2		Phe^{183}	Stack
		Phe^{259}	Stack
	O3	Lys^{232} N-ζ	3.0
Subsite -1	O2	His^{233} N-ε2	2.7
		Phe^{259} N	w.m.
		Glu^{257} O	w.m.
	O3	Glu^{257} O-ε1	3.0
Subsite 1		Tyr^{100}	Stack
	N1 (scissile bond)	Glu^{257} O-ε1	2.8
		Glu^{257} O-ε2	3.2
	O2	Asp^{328} O-δ2	2.9
		His^{327} N-ε2	2.7
	O3	Asp^{328} O-δ	3.2
	O6	Asp^{229} O-δ2	2.9
		His^{140} N-ε2	2.8
Subsite 2	O2	Arg^{375} NH1	2.7
	O3	Asp^{371} O-δ1	2.7
	O6	Trp^{101} N-ε1	2.7
Subsite 3	O2	Lys^{47} N-ζ	3.2

Our first approach was to design a mutation that would hinder the maltononaose binding mode and possibly bind a substrate in the maltohexaose conformation. We found that the replacement of Asp^{197} by His fulfilled these requirements, since modeling of the mutation D197H (Fig. 4) shows that the His ring cannot assume a conformation in which all the atoms are more than 2.0 Å away from the atoms in the maltononaose inhibitor. So His^{197} is likely to block the straight conformation. Moreover, the His^{197} N-ε2 atom could potentially stabilize the bent conformation by forming a hydrogen bond with the glucoside O6 at subsite +3. The D197H mutation changes the electrostatic field of the active site, which could have long distance effects by changing charge-charge interactions. However, since the substrate is uncharged, effects on the substrate binding

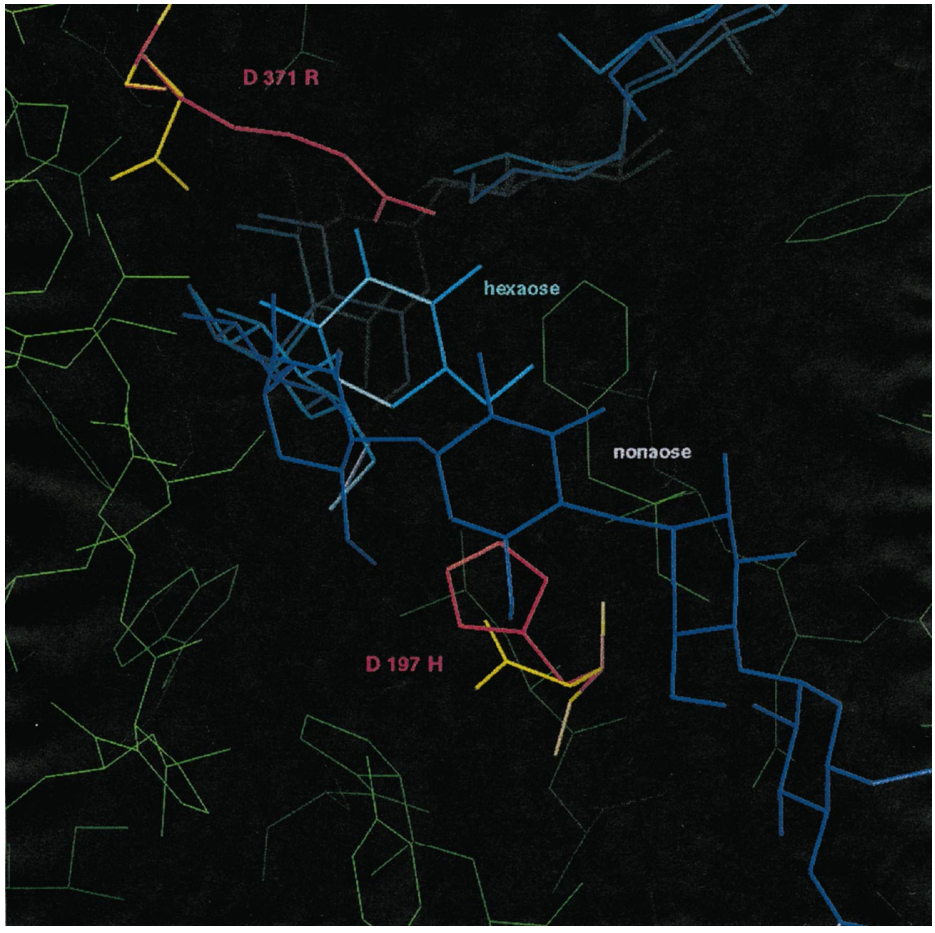

FIG. 4. **Model of the mutations D371R and D197H in the CGTase from *T. thermosulfurigenes* EM1 (*green* and *yellow*) together with the maltohexaose structure.** The mutations (*red*) have been given the most frequently occurring side chain conformation (with O; Ref. 28) that doesn't involve steric clashes with the enzyme. The maltohexaose chain is depicted in *light blue*; the modeled maltononaose chain in the *B. circulans* 251 CGTase structure is colored *dark blue*.

mode will have to be indirect, in contrast to the van der Waals and hydrogen bonding interactions.

Our second approach was to construct a mutant that would stimulate the maltononaose conformation over the maltohexaose conformation, which is easiest achieved, not by constructing a specific interaction with the straight conformation, but by destabilizing the bent conformation. With the mutation Asp^{371} to Arg we aimed at introducing a bulky residue that would clash with the maltohexaose conformation, but be less hindering to the straight maltononaose conformation (Fig. 4). The long and flexible side chain of Arg^{371} could probably extend its effect to subsite +3, where the bent and straight conformations differ most. The mutation D371R changes again the electrostatics of the active site, with possible indirect consequences for substrate binding. However, the mutation conserves the polarity of residue 371.

Of the two mutants D197H, designed to relatively stabilize the maltohexaose conformation, is expected to produce more α-cyclodextrin. Mutant D371R, designed to prefer the maltononaose conformation, is expected to produce less α-cyclodextrin. The experimental data show that these mutants display altered cyclodextrin product specificity according to expectation (Table III).

Production and Purification of CGTase (Mutant) Proteins

Mutants of *Tabium* CGTase were successfully constructed by site-directed mutagenesis via PCR; all mutations were verified by restriction site analysis (except for mutant F284K) and DNA sequencing. Amounts of 0.4–1.2 mg of pure protein were obtained in a single fermentor run depending on the construct used (Table IV). Purification yields varied between 11% for mutant D371R and 58% for mutant D197H. Purity and molecular weight of the (mutant) CGTases were checked on SDS-polyacrylamide gel electrophoresis. All proteins were purified to apparent homogeneity and displayed a molecular mass of 68 kDa.

Characterization of CGTase Mutant Proteins

Cyclodextrin Product Specificity—Mutant D197H has a cyclodextrin production profile different from wild-type CGTase (Fig. 5). At the initial stages of the reaction, the mutant has an increased preference for α-cyclodextrin production, mostly due to a collapse of the production of β-cyclodextrin. At later stages of the reaction, the production of β-cyclodextrin increases, but the product ratio is then a result of a subtle equilibrium between cyclization and cyclodextrin breakdown specificities, as well as the solubilities of the diverse cyclodextrins. However, the cyclodextrin production ratio after 45 h still shows a small preference for α-cyclodextrin (Table III), proving that the total product ratio can be modified by changing the initial reaction rates. The initial reaction's preference for α-cyclodextrin is according to the expectations we had upon designing the mutant (see above). An additional effect of the mutation D197H is that coupling activity is reduced by a factor 4 when compared with the activity of the wild-type enzyme (Table V), possibly because coupling activity was measured with β-cyclodextrin whereby a maltononaose was formed as an intermediate. The mutation was, however, designed to make binding of maltononaose less favorable.

Mutant D371R displayed drastically decreased cyclization, coupling, disproportionation and saccharifying activities when compared with the wild-type enzyme (Table V). Asp^{371} has a very important role in substrate binding at subsite +2, both in the *BC251* and *Tabium* CGTase (Table II; Ref. 13). When Asp^{371} is replaced by Arg, the bulk of the residue could hamper efficient substrate binding at subsite +2 and the charge difference could interfere with the catalytic process in site +1, resulting in having an overall activity of only 9% of the wild-type CGTase (Table V). However, not the efficiency of the catalytic process is determining product specificity, but the preference for forming a specific intermediate leading to a specific product at an initial stage in the CGTase reaction. The product specificity changed from 28:58:14 for the wild-type enzyme to 6:68:26 for mutant D371R (Table III, Fig. 5). This suggests that the intermediate specific for α-cyclodextrin production in the cyclization reaction of the mutant D371R is less frequently formed. As pointed out above, we think that this intermediate has a conformation resembling the maltohexaose "bent" conformation, formation of which could be sterically hindered by the bulky Arg^{371} residue.

These results lend more credence to the theory that the bent conformation is correlated with α-cyclodextrin production and show that it can be used to rationally engineer a CGTase with desired cyclodextrin product specificity (12). The results show that the *Tabium* CGTase can be changed from an α/β-cyclodextrin producer to a β/γ-cyclodextrin producer by just one mutation. We currently are working on a wider range of mutations and a more detailed thermodynamical and structural characterization of them to further investigate the significance of the bent conformation and other structure-function relationships in CGTase.

Site-directed Mutations Close to the Proton Donor Glu^{258}: Implications for pH Optima of CGTases—To further investigate the role of the environment of Glu^{258} on the pK_a of Glu^{258}

TABLE III
Starch conversion of T. thermosulfurigenes wild-type and mutant CGTase proteins

Proteins (0.1 unit/ml β-CD forming activity) were incubated for 45 h at pH 6.0 and 60 °C with 10% Paselli WA4.

CGTase	Conversion of starch into cyclodextrins	Product ratio			Conversion of starch into G1–G3
		α	β	γ	
	%		%		%
Wild-type	35	28	58	14	11
D197H	37	35	49	16	15
F284K	27	31	58	11	20
N327D	13	24	62	14	7
D371R	29	6	68	26	2

TABLE IV
Purification of T. thermosulfurigenes wild-type and mutant CGTase proteins from E. coli PC1990 culture supernatants

	Supernatant[a]		Purified protein fractions				
	Specific activity[b]	Total activity[b]	Specific activity[b]	Total activity[b]	Purification factor	Yield	Pure protein
	units/mg	*units*	*units/mg*	*units*	*-fold*	*%*	*mg*
Wild-type	0.80	300	163	78	204	26	0.6
D197H	0.69	300	144	173	209	58	1.2
F284K	1.24	540	86	103	69	19	1.2
N327D	0.32	170	51	51	159	30	1.0
D371R	0.15	56	14	14	93	11	0.4

[a] 2-Liter supernatant was used for purification of the proteins.
[b] β-Cyclodextrin forming activities are shown.

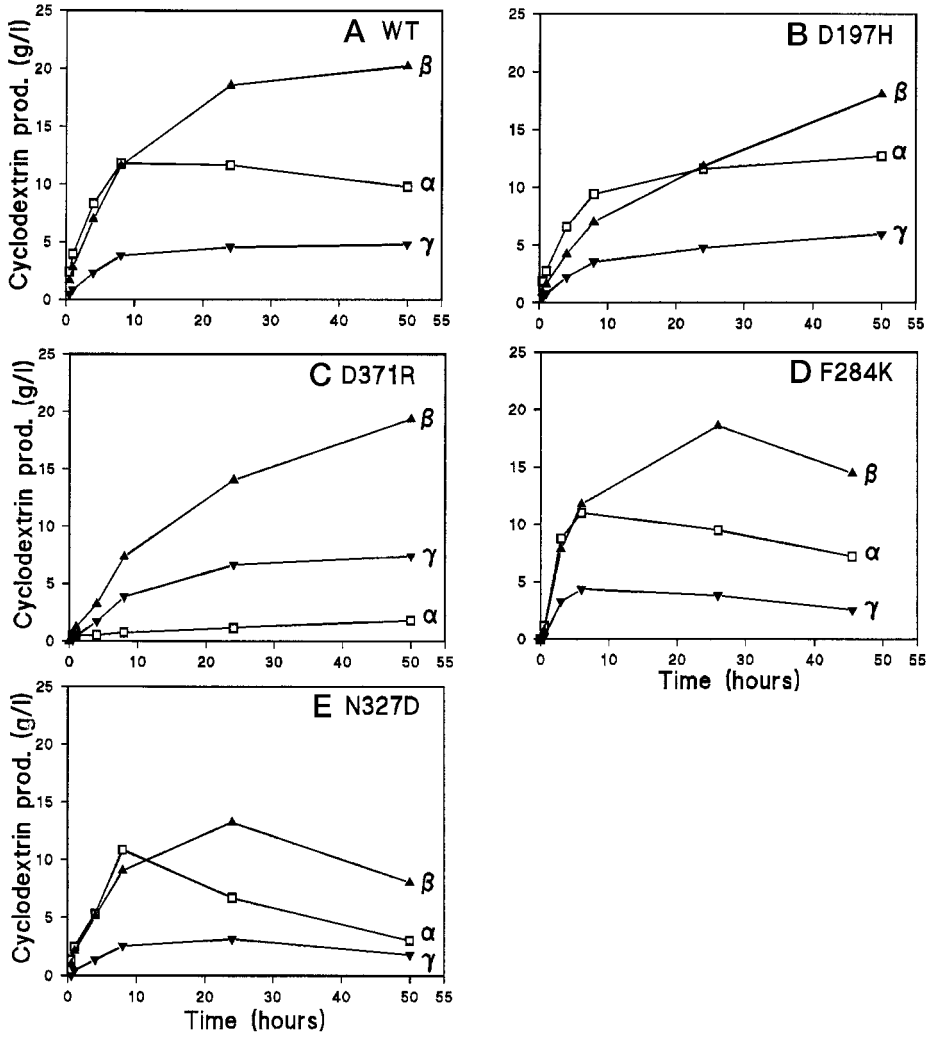

FIG. 5. **Cyclodextrins formed during incubation of (mutant) CGTase proteins from *T. thermosulfurigenes* EM1 (0.1 unit/ml β-CD forming activity) with 10% (w/v) Paselli WA4 starch for 50 h at pH 6.0 and 60 °C.** □, α-CD; ▲, β-CD; ▼, γ-CD. *A*, wild-type CGTase; *B*, mutant D197H; *C*, mutant D371R; *D*, mutant F284K; *E*, mutant N327D.

TABLE V
Specific enzyme activities and pH optima for activity of T. thermosulfurigenes EM1 wild-type and mutant CGTase proteins

	Specific enzyme activities				pH optima	
	Cyclization[a]	Coupling	Disproportionation	Saccharifying[b]	Cyclization	Saccharifying[b]
	units/mg					
Wild-type	163	46	332	24	4.5–6.5	4.0–5.0
D197H	144	11	411	17	5.5–6.0	4.0–5.0
F284K	86	23	455	8	4.5–6.0	3.0–3.5
N327D	51	4	318	18	4.5–5.5	3.0–3.5
D371R	14	0.2	36	<0.01	4.5–5.5	ND[c]

[a] β-CD forming activities are shown.
[b] Hydrolysis is measured as saccharifying activity.
[c] Not determined.

in the different reactions catalyzed by CGTases we replaced Phe^{284} by Lys (F284K) in *Tabium* CGTase. Residue Phe^{284} is located in a hydrophobic cavity immediately above the active site, close to Glu^{258} (Fig. 6). At most physiological pH values Lys can be expected to bear a positive charge. Positioning of a positive charge near Glu^{258} stabilizes its deprotonated form, so decreasing its pK_a. This would predict a shift of the pH optimum for this mutant toward acidity. Fig. 7, *A* and *B*, show that this indeed happens for both the cyclization and hydrolysis activity. Apart from this effect, the optimum curves also become more narrow, an observation that was also made for a F184L mutant in *Bacillus* sp. 1011 CGTase (18). The mutation F184L does not introduce any charges; therefore, the narrowing effect can be best explained by a reduction of the hydrophobicity of the environment of Glu^{258} (see below).

Residue Asn^{327} is also situated above the active site, close to Glu^{258} (Fig. 6). Mutation N327D in *T. thermosulfurigenes* CGTase introduced a group that can bear a negative charge at high pH next to Glu^{258}. This would increase the pK_a of Glu^{258} by destabilizing its deprotonated form. A shift of the pH optimum toward alkaline regions is expected. However, we observe that both cyclization and hydrolysis optima shift to lower pH (Fig. 7, *A* and *B*). A similar loss of activity at high pH has been observed in a N327D mutant of *Bacillus stearothermophilus* α-amylase, an enzyme homologous to CGTase (21). A N327V mutant of the same enzyme remained active at high pH, suggesting that the effects of mutations N327D are due specifically to introduction of an acidic group.

A possible explanation for the observed shift of activity to acidic regions for mutant N327D of *T. thermosulfurigenes* CG-

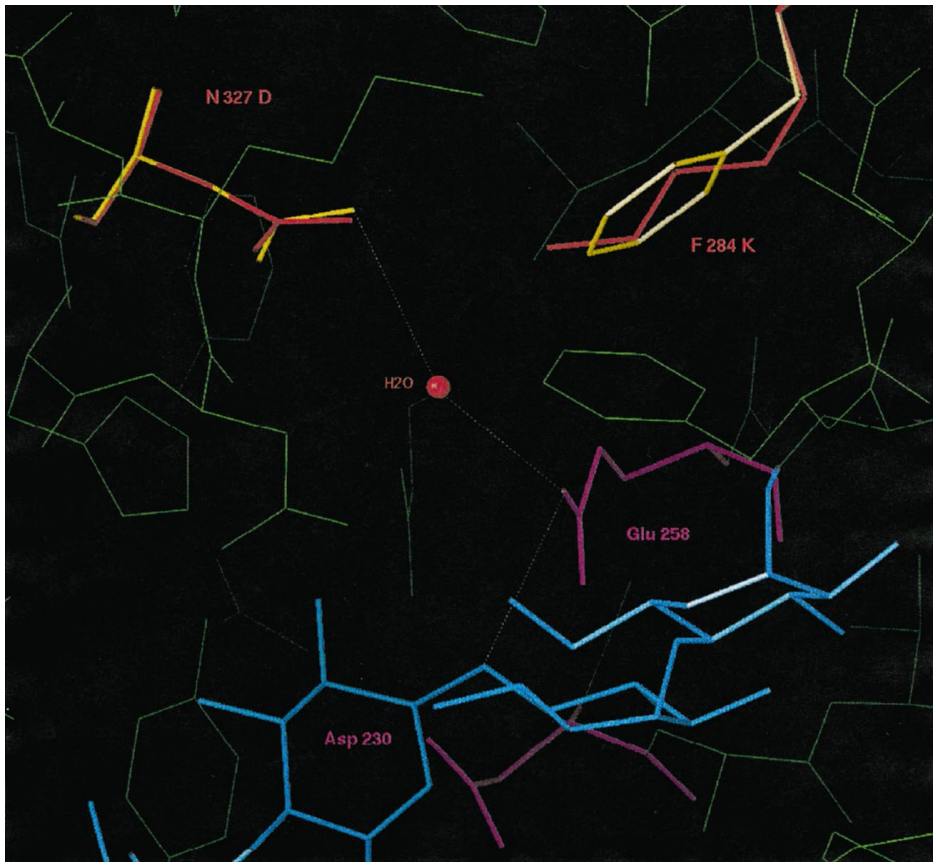

FIG. 6. **Model of the mutations near Glu^{258}.** Residues in the CGTase from *T. thermosulfurigenes* EM1 are shown in *green* and *yellow*. The maltohexaose structure is given in *blue*. The mutations N327D and F284K are modeled in *red*, as described in the legend to Fig. 4. The *red sphere* is the water as mentioned in the text.

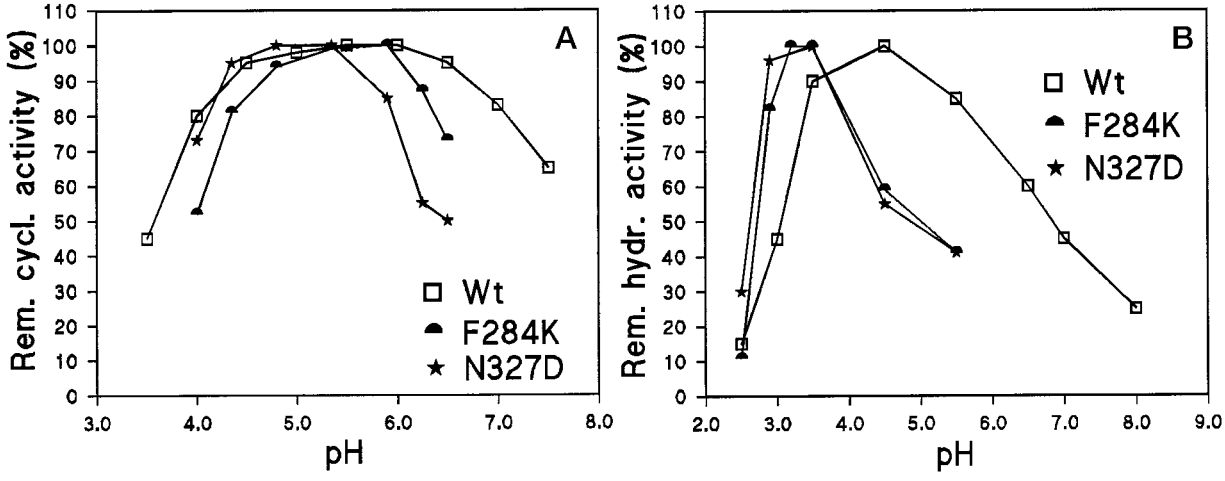

FIG. 7. *A*, effect of pH on the cyclization activity of CGTase (mutant) proteins from *T. thermosulfurigenes* EM1. *B*, effect of pH on the saccharifying activity of the CGTase (mutant) proteins from *T. thermosulfurigenes* EM1.

Tase can be found by observing that Asn^{327} binds Glu^{258} via a water molecule (Fig. 6) and is secluded from the bulk solvent by hydrophobic residues such as Phe^{284}, Phe^{324}, Phe^{260}, Met^{330}, and Leu^{282}. In such an environment, the Asp^{327} and the water molecule would form a very stable salt bridge between the negatively charged carboxylate group and a H_3O^+ ion. Because the H_3O^+ ion is closest to Glu^{258}, the net effect of the mutation would be to bring a positive charge close to Glu^{258}, resulting in an overall decrease of its pK_a. This would explain why the behavior of the N327D and F284K mutations are so alike.

Cyclodextrin product ratios of mutants F284K and N327D were not significantly changed compared with the wild-type enzyme, which might be expected, since both residues are not involved in substrate binding (Table V). All specific enzyme activities were decreased for mutants F284K and N327D compared with the wild-type activities, except for the disproportionation activity of F284K (Table III). Mutations near the proton donor thus have an overall negative effect on catalysis rates.

pH Optimum Curve for Cyclization and Hydrolysis—In *Tabium* CGTase residue Glu^{258} is the proton donor in the first step of catalysis, so a protonated state of Glu^{258} is essential. In the second step of catalysis, Glu^{258} is suggested to activate the acceptor by deprotonation, in this case a deprotonated state of Glu^{258} would be essential. Furthermore, for optimal activity the catalytic nucleophile, Asp^{230}, must remain deprotonated in the first step of catalysis. The *Tabium* CGTase displays a broad pH optimum for cyclization in the range of pH 4–7 (Fig. 7*A*). Other CGTases have an efficient cyclization reaction from pH 5 to 7 (16, 18, 21, 22). It might be expected that the drop in

enzyme activity at high pH is caused by deprotonation of Glu^{258} in the first step of the reaction and that the activity drop at low pH is caused by protonation of Asp^{230}. The combination of these two effects would result in a pH optimum curve. In Fig. 7*A*, however, it can be seen that the mutations near Glu^{258} shift both the slopes at high and low pH, while we had expected only to see effects on the high pH slope of the optimum curve, which is affected by Glu^{258}. Similar observations have been described before in literature. The mutation F284L in *Bacillus* sp. 1011 CGTase shifts the pH optimum both over acidic and alkaline pH ranges (18). This mutation is close to the proton donor and is unlikely to have long distance effects. Mutation of Asp^{329} in *BC251* CGTase to Asn had a most pronounced effect on the low pH slope of the optimum curve (20). Furthermore, mutation of Asp^{230} to Asn in the *BC251* CGTase did not result in any shift of the pH optimum, whereas a shift was observed with the Glu^{258} to Gln mutation (20). Therefore, it is likely that the protonation state of Glu^{258} determines both slopes of the pH optimum curve. At high pH, the first step of the double displacement mechanism is hindered by lack of a proton donor, at low pH the second step is inhibited by incomplete substrate activation. If the protonation state of Glu^{258} determines both slopes of the pH profile, it is unexpected that the pH optimum is so broad. This broad pH range of activity must be explained by a different environment for Glu^{258} in the first and second step of catalysis. Indeed, in *Tabium* CGTase (6) the third catalytic residue Asp^{329} probably forms a hydrogen bond with Glu^{258} initially, increasing the pK_a of Glu^{258} and ensuring its protonation. This bond is broken after substrate binding, facilitating again deprotonation of Glu^{258} in the ensuing second catalytic step. The impact of changes near Glu^{258} during catalysis is enhanced by its hydrophobic environment, in which electrostatic interactions are much stronger. Changes in the environment of Glu^{258} before and after substrate binding have also been observed in the structure of *BC251* CGTase (13, 16).

The pH optimum for hydrolysis is much sharper and lies about 1 pH unit lower than the pH optimum for cyclization in the *Tabium* CGTase (Fig. 7*B*). The only difference between these two reactions is the acceptor molecule, water in the hydrolysis reaction, and a C4-hydroxyl group in the cyclization reaction. The fact that the pH optimum for hydrolysis is less broad could result from a decreased hydrophobicity of the Glu^{258} environment with water as an acceptor. The shift toward lower pH might be explained from the fact that water as an acceptor is much easier activated, making the requirement for an unprotonated Glu^{258} in the second reaction step less stringent, thus increasing activity at low pH.

CONCLUSIONS

At subsite 3 the binding mode of the maltohexaose inhibitor in *Tabium* CGTase is radically different from the maltononaose binding mode in the *BC251* CGTase. The bent conformation of the maltohexaose inhibitor, in contrast to the straight conformation of the maltononaose inhibitor, was found to be correlated to enhanced α-cyclodextrin production. Mutations stabilizing the bent conformation but hindering the straight conformation resulted in enhanced production of α-CD, whereas mutations hindering the bent conformation but stabilizing the straight conformation resulted in decreased production of α-CD. The *Tabium* CGTase can hence be changed from an α/β-cyclodextrin producer to a β/γ-cyclodextrin producer by a single mutation, illustrating the feasibility of CGTase protein engineering.

Mutations near the proton donor Glu^{258} suggest that the pH optimum curve of CGTase may be determined only by the protonation state of residue Glu^{258}. Both the high and low slopes of the pH optimum curve could be manipulated by site-directed mutations close to Glu^{258}. Changes in the environment of Glu^{258} before and after substrate binding can account for its broad pH optimum.

Acknowledgments—The assistance of Dirk Penninga, Jan Springer, and Gerard Rouwendaal with construction of the mutants and the assistance of Gert-Jan van Alebeek with the enzyme assays is gratefully acknowledged.

REFERENCES

1. Schmid, G. (1989) *Trends Biotechnol.* **7,** 244–248
2. Starnes, R. L. (1990) *Cereal Foods World* **35,** 1094–1099
3. Pedersen, S., Dijkhuizen, L., Dijkstra, B. W., Jensen, B. F., and Jörgensen, S. T. (1995) *Chemtech* Dec 19–25
4. Klein, C., and Schulz, G. E. (1991) *J. Mol. Biol.* **217,** 737–750
5. Lawson, C. L., van Montfort, R., Strokopytov, B., Rozeboom, H. J., Kalk, K. H., de Vries, G. E., Penninga, D., Dijkhuizen, L., and Dijkstra, B. W. (1994) *J. Mol. Biol.* **236,** 590–600
6. Knegtel, R. M. A., Wind, R. D., Rozeboom, H. J., Kalk, K. H., Buitelaar, R. M., Dijkhuizen, L., and Dijkstra, B. W. (1996) *J. Mol. Biol.* **256,** 611–622
7. Harata, K., Haga, K., Nakamura, A., Aoyagi, M., and Yamane, K. (1996) *Acta Crystallogr. Sect. D* **52,** 1136–145
8. Svensson, B. (1994) *Plant Mol. Biol.* **25,** 141–157
9. Starnes, R. L. (July 11, 1991) International Patent WO 91/09962
10. Norman, B. E., and Jörgensen, S. T. (1992) *Denpun Kagaku* **39,** 101–108
11. Wind, R. D., Liebl, W., Buitelaar, R. M., Penninga, D., Spreinat, A., Dijkhuizen, L., and Bahl, H. (1995) *Appl. Environ. Microbiol.* **61,** 1257–1265
12. Dijkhuizen, L., Dijkstra, B. W., Andersen, C., and von der Osten, C. (October 24, 1996) International Patent WO96/33267
13. Strokopytov, B., Knegtel, R. M. A., Penninga, D., Rozeboom, H. J., Kalk, K. H., Dijkhuizen, L., and Dijkstra, B. W. (1996) *Biochemistry* **35,** 4241–4249
14. Penninga, D., Strokopytov, B., Rozeboom, H. J., Lawson, C. L., Dijkstra, B. W., Bergsma, J., and Dijkhuizen, L. (1995) *Biochemistry* **34,** 3368–3376
15. Koshland, D. E. (1953) *Biol. Rev. Camb. Philos. Soc.* **28,** 416–436
16. Strokopytov, B., Penninga, D., Rozeboom, H. J., Kalk, K. H., Dijkhuizen, L., and Dijkstra, B. W. (1995) *Biochemistry* **34,** 2234–2240
17. Davies, G., and Henrissat, B. (1995) *Structure* **3,** 853–859
18. Nakamura, A., Haga, K., and Yamane, K. (1994) *Biochemistry* **33,** 9929–9936
19. Takase, K. (1993) *Eur. J. Biochem.* **211,** 899–902
20. Knegtel, R. M. A., Strokopytov, B., Penninga, D., Faber, O. G., Rozeboom, H. J., Kalk, K. H., Dijkhuizen, L., and Dijkstra, B. W. (1995) *J. Biol. Chem.* **270,** 29256–29264
21. Fujiwara, S., Kakihara, H., Sakaguchi, K., and Imanaka, T. (1992) *J. Bacteriol.* **174,** 7478–7481
22. Klein, C., Hollender, J., Bender, H., and Schulz, G. E. (1992) *Biochemistry* **31,** 8740–8746
23. Kabsch, W. (1993) *J. Appl. Crystallogr.* **26,** 795–800
24. Tronrud, D. E., Ten Eyck, L., and Matthews, B. W. (1987) *Acta Crystallogr. Sect. A* **43,** 489–501
25. Brünger, A. T. (1993) *Acta Crystallogr. Sect. D* **49,** 24–36
26. Engh, R. A., and Huber, R. (1991) *Acta Crystallogr. Sect. A* **47,** 392–400
27. Takusagawa, F., and Jacobson, R. A. (1978) *Acta Crystallogr. Sect. B* **34,** 213–218
28. Jones, T. A., Zou, J. Y., Cowan, S. W., and Kjeldgaard, M. (1991) *Acta Crystallogr. Sect. A* **47,** 110–119
29. Kleywegt, G. J., and Jones, T. A. (1994) *ESF/CCP4 Newsletter*, Vol. 30, pp. 20–24
30. Read, R. J. (1986) *Acta Crystallogr. Sect. A* **42,** 140–149
31. Bhat, T. N. (1988) *J. Appl. Crystallogr.* **21,** 279–281
32. Qian, M., Haser, R., Buisson, G., DuJe, E., and Payan, F. (1994) *Biochemistry* **33,** 6284–6294
33. Lamzin, V. S., and Wilson, K. S. (1993) *Acta Crystallogr. Sect. D* **49,** 129–147
34. Laskowski, R. A., MacArthur, M. W., Moss, D. S., and Thornton, J. M. (1993) *J. Appl. Crystallogr.* **26,** 283–291
35. Yanisch-Perron, C., Vieira, J., and Messing, J. (1985) *Gene* (*Amst.*) **33,** 103–119
36. Lazzaroni, J. C., and Portalier, R. (1979) *FEMS Microbiol. Lett.* **5,** 411–416
37. Haeckel, K., and Bahl, H. (1989) *FEMS Microbiol. Lett.* **60,** 333–338
38. Sambrook, J., Fritsch, E. J., and Maniatis, T. (1989) *Molecular Cloning: A Laboratory Manual*, Cold Spring Harbor Laboratory, Cold Spring Harbor, NY
39. Sanger, F., Nicklen, S., and Coulsen, A. R. (1977) *Proc. Natl. Sci. U. S. A.* **74,** 5463–5467
40. Monma, M., Mikuni, K., and Kainuma, K. (1988) *Biotechnol. Bioeng.* **32,** 404–407
41. Nakamura, A., Haga, K., and Yamane, K. (1993) *Biochemistry* **32,** 6624–6631
42. Bradford, M. M. (1976) *Anal. Biochem.* **72,** 248–254
43. Penninga, D. (1996) *Protein Engineering of Cyclodextrin Glycosyltransferase from Bacillus circulans Strain 25.* Ph.D. thesis, Ponsen & Looÿen B.V., Wageningen, The Netherlands